Annals of Physics 398 (2018) 180–189

Contents lists available at ScienceDirect

Annals of Physics

journal homepage: www.elsevier.com/locate/aop

Localization properties and high-fidelity state transfer in hopping models with correlated disorder

G.M.A. Almeida *, C.V.C. Mendes, M.L. Lyra, F.A.B.F. de Moura

Instituto de Física, Universidade Federal de Alagoas, Maceió AL 57072-970, Brazil

ARTICLE INFO

Article history:
Received 30 November 2017
Accepted 3 September 2018
Available online 6 September 2018

Keywords:
Correlated disorder
Localization
Quantum-state transfer

ABSTRACT

We investigate a tight-binding chain featuring diagonal and off-diagonal disorder, these being modeled through the long-range-correlated fractional Brownian motion. Particularly, by employing exact diagonalization methods, we evaluate how the eigenstate spectrum of the system and how its related single-particle dynamics respond to both competing sources of disorder. Moreover, we report the possibility of carrying out efficient end-to-end quantum-state transfer protocols even in the presence of such generalized disorder due to the appearance of extended states around the middle of the band in the limit of strong correlations.

© 2018 Elsevier Inc. All rights reserved.

1. Introduction

In the past few decades, there has been a growing interest in investigating quantum transport properties of low dimensional disordered lattices [1–16], most of them based on Anderson scaling theory. In general lines, it is well established that there are no extended eigenstates in low-dimensional systems for any amount of uncorrelated disorder. The breakdown of standard Anderson localization theory was put forward about thirty years ago by Flores and Dunpap [17,18]. They pointed out that the presence of short-range correlations in the disorder distribution yielded the appearance of extended states in the spectrum of disordered chains. That could explain to a great extent some unusual transport properties of several types of polymers [17,18]. Right after this discovery, a handful of works came along to investigate the role of disorder correlations, either short- or long-ranged, in a wide variety of physical systems [19–40]. Particularly, it was shown in

* Corresponding author.
E-mail address: dealmeidagma@gmail.com (G.M.A. Almeida).

https://doi.org/10.1016/j.aop.2018.09.003
0003-4916/© 2018 Elsevier Inc. All rights reserved.

Refs. [19,21] that long-range correlated random potentials can actually allow for mobility edges in 1D disordered models. In Ref. [19], that specific kind of fluctuations was generated using the trace of a fractional Brownian motion whose intrinsic correlations decay following a power-law. Through numerical renormalization methods, it was show that this model exhibits a phase of extended states around the center of the band [19]. Tackling the same problem, the authors in [21] applied an analytical perturbation technique and came up with a direct relationship between the localization length and the characteristics of the intrinsic correlations in the disorder distribution. A few years later, the above results were validated through experiments carried out in microwave guides featuring correlated scatters [41]. The authors demonstrated that intrinsic long-range correlations within the scatters distribution ultimately improve the wave transmission. On the theoretical side, the Anderson model with long-range correlated hopping fluctuations (off-diagonal disorder) was studied in Refs. [20,32]. Likewise, it was found that strong correlations promote the appearance of a phase of extended states close to the center of the band.

In this work we provide further progress along those lines. In particular, we consider two sources of disorder acting simultaneously on the potentials as well as on the hopping strengths of the chain, both exhibiting long-range correlated fluctuations generated by the fractional Brownian motion. This model embodies a generalized disordered scenario which we aim to push on its capability of supporting extended states in the middle of the band thereby weakening Anderson localization. By looking at the participation ratio of eigenstates and also at the dynamics of the system through its mean square displacement for a delta-like initial state we find out that the chain allows for propagating modes if substantial long-range correlations are taking place in both sources of disorder. Looking forward possible applications in the field of quantum-information processing, we also investigate whether such a model of generalized disorder would allow for realizing standard quantum-state transfer protocols [42–49], particularly those relying on weak-coupled parties [44–46,48]. The point is that when designing chains for transmitting quantum states from one point to another – which is a crucial requirement in quantum networks [50] –one should take into account the possibility of undesired fluctuations taking place due to experimental errors [40,46,51–58], that including correlated noise [40,51,52,58]. Our calculations reveal that an electron (or a properly encoded qubit) can be almost fully transferred through the noisy bulk of the chain depending upon specific sets of parameters.

2. Model and formalism

We consider a N-site linear chain described by the electronic tight-binding Hamiltonian ($\hbar = 1$)

$$H = \sum_{n=1}^{N} \epsilon_n |n\rangle\langle n| + \sum_{n=1}^{N-1} J_n (|n\rangle\langle n+1| + \text{h.c.}), \tag{1}$$

written in the Wannier basis set $\{|n\rangle\}$ accounting for the electron position, where ϵ_n is the on-site potential and J_n is the hopping strength, those being the source of static disorder. Those parameters are here expressed in terms of energy unit $J \equiv 1$. Specifically, we assume that both quantities fluctuate such that their corresponding disorder distributions come with intrinsic long-range correlations modeled via the fractional Brownian motion [19,22,24,25]

$$\epsilon_n, J_n = \sum_{k=1}^{N/2} \frac{1}{k^{\gamma/2}} \cos\left(\frac{2\pi nk}{N} + \phi_k\right). \tag{2}$$

We emphasize that the sequence generated by the equation above exhibits a power-law spectrum $1/k^{\gamma}$ and ϕ_k represents a random phase uniformly distributed within the range $[0, 2\pi]$. For $\gamma = 0$, the sequence is fairly uncorrelated. On the other hand, $\gamma > 0$ brings about long-range correlations in the disorder sequence. Therefore, exponent γ stands out as a very important parameter since it controls the *degree* of correlations within the disordered sequence. Hereafter, Eq. (2) will be used for generating disorder distributions for both ϵ_n and J_n but with a few remarks: (i) for ϵ_n we attribute $\gamma \to \alpha$ and normalize the entire sequence so that $\langle \epsilon_n \rangle = 0$ and $\langle \epsilon_n^2 \rangle = 1$; (ii) for J_n we set $\gamma \to \beta$ and

redefine $J_n \to \tanh(J_n)+2$ after normalization in order to rule out possible null hopping strengths. It is also important to note that each sequence for ϵ_n and J_n is generated using distinct sets of phases, $\{\phi_k\}$. In summary, the model contains two *independent* parameters α and β that account for the degree of correlations for both diagonal and off-diagonal sources of disorder.

The quantities of interest are all obtained through exact diagonalization of Hamiltonian (1) which gives us the eigenvalues $\{E_j\}$ and its corresponding eigenvectors $|\psi^j\rangle = f_n^j|n\rangle$. Our first task will be evaluating the participation ratio defined as [24]

$$\xi^j = \frac{1}{\sum_n |f_n^j|^4}. \tag{3}$$

This measure provides an estimate of the number of bare states a given eigenstate is spread on, i.e., it quantifies the degree of localization. In particular, the participation number becomes size-independent for localized wave-packets and diverges with N for extended ones. In addition, we investigate the electronic time evolution through the chain. We initialize the initial wave-packet in $|\psi(0)\rangle = \sum_n c_n(0)|n\rangle$ where $c_n(0) = \delta_{n,n_0}$. The electronic state at time t can thus be obtained from $|\psi(t)\rangle = \sum_n c_n(t)|n\rangle = e^{-iHt}|\psi(0)\rangle$, where

$$c_n(t) = \sum_j f_{n_0}^{j*} f_n^j e^{-iE_j t}. \tag{4}$$

By using the relations above we can compute the width σ of the electronic wave-packet through [59]

$$\sigma(t) = \sqrt{\sum_n (n - \langle n(t)\rangle)^2 |c_n(t)|^2}, \tag{5}$$

where $\langle n(t)\rangle = \sum_n n|c_n(t)|^2$ is the electronic average position. Note that $\sigma(t)$ goes from 0, for a wave function confined to a single site, to $O(N)$ for a wave extended over the whole system. Note that we can also compute the time-dependent participation number defined as $\xi(t) = 1/\sum_n |c_n(t)|^4$. Both quantities are distinct ways to obtain an estimate of the size of the wave-packet at time t [24,59].

3. Results

After having introduced the main tools in the previous section, we now provide a detailed investigation of the actual role played by diagonal and off-diagonal sources of disorder acting simultaneously in the chain.

3.1. Localization properties

We start our analysis showing results for the participation ratio of the entire eigenstates set. It should be emphasized that every quantity evaluated in this work was properly averaged over many distinct realizations of disorder. The total number of eigenstates $N_E = NM$ was larger than 10^5 for all calculations, M being the number of samples. We averaged ξ^j over a small window around energy E and therefore we are looking towards the quantity $\xi(E) = (\sum_{E_j>E-\Delta E}^{E_j<E+\Delta E} \xi^j)/n(E)$, where $n(E)$ is the number of eigenvalues $\{E_j\}$ within the interval $[E-\Delta E, E+\Delta E]$. Herein we fix $\Delta E = 0.2$ which was chosen much smaller than the total bandwidth but large enough to contain a large number of eigenstates to produce a good statistical average.

In Fig. 1(a)–(c) we plot the rescaled mean participation number ξ/N versus energy E for many combinations of α and β. Calculations were done for $N = 1000$ up to 8000 sites. We observe in Fig. 1(a) and (b) that ξ/N decreases as the system size N is increased regardless of the E value. That is a clear signature that all eigenstates become localized in the thermodynamic limit. On the other hand, Fig. 1(c) reveals a rather interesting behavior. Close to the band center, the rescaled participation number remains constant thus indicating the appearance of extended states at this region. For $|E| \gg 0$ we observe that ξ/N decreases slowly with N what indicates the presence of localized states far from the band center. However, these localized states are not size independent,

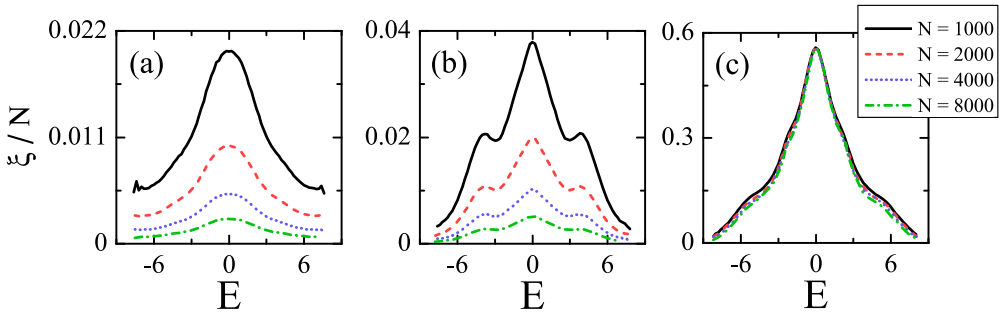

Fig. 1. Rescaled participation number ξ/N versus E for (a) $\alpha = 3$, $\beta = 0$; (b) $\alpha = 0$, $\beta = 3$; and (c) $\alpha = 3$, $\beta = 3$ for several system sizes. Notice that for $\alpha = \beta = 3$ delocalized states appear near the band center.

as it is usual in systems with uncorrelated disorder. They depict a sub-linear scaling due to the size-dependent rescaling of the coupling constants [60]. The size dependence of the participation number for some typical energies is shown in Fig. 2(a). In order to clearly locate the mobility edges in the case of strong disorder, the normalized localization length L/N is a more appropriate measure. The localization length L was obtained using a standard transfer matrix formalism (cf. Ref. [2] for details). Even in the regime of weak localization with power-law growth of the participation number, the localization length remains finite because it is mainly associated with the behavior of the eigenstates on their exponentially decaying tails. In Fig. 2(b) we report the spectrum of the normalized localization length for $\alpha = \beta = 3$ which clearly signals the mobility edges. Thereby, our calculations show that one-dimensional systems featuring both diagonal and off-diagonal disorder only display extended states whenever both sources of fluctuations are augmented with strong long-range correlations. If only either α *or* β is greater than zero, the electron transport can be suppressed by the presence of uncorrelated randomness in the lattice.

We can further observe that feature by analyzing Fig. 3, where we plot the mean participation number around the band center $\xi_0/N \equiv \xi(E \approx 0)/N$ versus α and β for $N = 8000$. We note that only for α *and* β larger than 2 we obtain the rescaled participation number $\xi_0/N \approx 0.58(2)$ which is very close to the corresponding value of extended states in ordered chains with open-boundary conditions, that is 2/3. Our outcomes are also in agreement with the rescaled participation number for extended states in disordered systems [22,24,32].

Furthermore, it is relevant to point out that, generally speaking, γ is related to the so-called Hurst exponent $\mathcal{H}$ through $\mathcal{H} = (\gamma - 1)/2$ which describes the long-term memory of a given series. The set spanned by Eq. (2) is said to be nonstationary when $\gamma > 1$ and persistent (anti-persistent) when $\gamma > 2$ ($\gamma < 2$). When $\alpha = 2$ the series corresponds exactly to the trace of the Brownian motion. $\mathcal{H} = 1$ for $\gamma \geq 3$ signaling that the generated series becomes locally completely correlated with no local roughness in the thermodynamic limit. However, global disorder still persists due to the random nature of the phases used to generate the full series. Moreover, as shown in [19] in the case of on-site disorder only, $\alpha = 2$ marks the transition point between Anderson-like insulator and metallic phases with sharp mobility edges.

3.2. Time dynamics and quantum-state transfer

The interplay between localized and delocalized states we have seen in the previous section allows for a rich variety of dynamical regimes [25]. Our goal now is explore how the competition between two independent sources of correlated disorder reflects upon the spreading profile of the initial state of a single electron. Right after that, we will tackle a very appealing application of such platforms in the context of quantum information processing.

Figs. 4 and 5 show a summary of our calculations for the time-dependent spread and participation number for an initial delta-like state prepared at the $(N/2)$th site, that is $c_n(0) = \delta_{n,N/2}$. Those

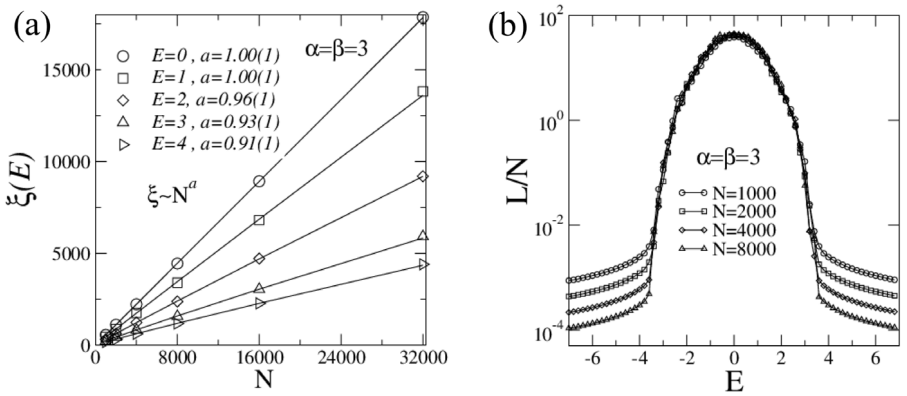

Fig. 2. In (a) we show the size dependence of the participation number for some typical energies evidencing the sub-linear scaling of the weakly localized states near the band edge. The spectrum of the normalized localization length L/N is shown in (b) which clearly signals the mobility edges. Here we fixed $\alpha = \beta = 3$.

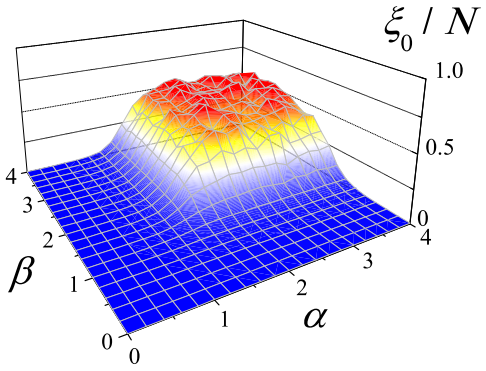

Fig. 3. Rescaled participation number around the band center, $\xi(E \approx 0)/N = \xi_0/N$, versus α and β for $N = 8000$ sites. The chain is able to support extended states around the center of the band only when both diagonal and off-diagonal sources of disorder are both long-range correlated obeying, roughly, $\alpha, \beta > 2$.

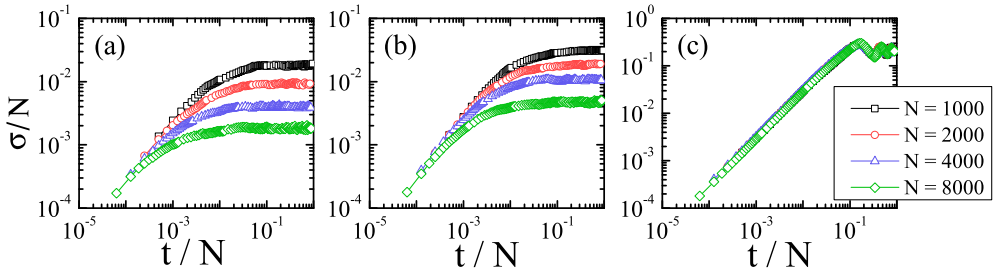

Fig. 4. Rescaled square root of the mean square displacement (σ/N) versus rescaled time (t/N) for (a) $\alpha = 3, \beta = 0$; (b) $\alpha = 0$, $\beta = 3$; and (c) $\alpha = 3$, $\beta = 3$.

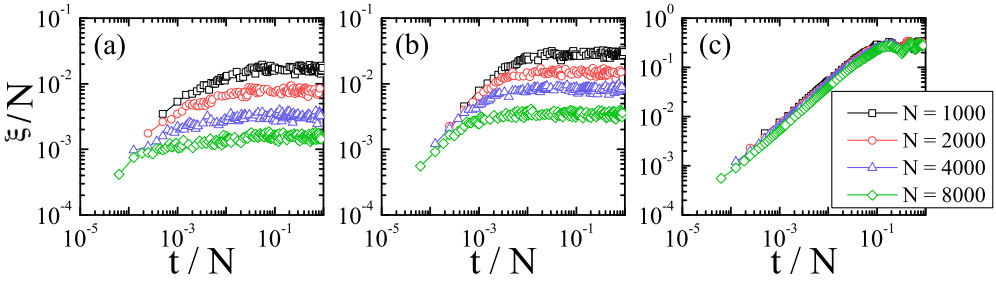

Fig. 5. Rescaled participation number (ξ/N) versus rescaled time (t/N) for (a) $\alpha = 3$, $\beta = 0$; (b) $\alpha = 0$, $\beta = 3$; and (c) $\alpha = 3$, $\beta = 3$.

coefficients at a later time are evaluated through Eq. (4) for $N = 1000$ up to 8000 for various combinations of α and β. For comparison purposes, time and functions of interest were rescaled by the system size N. We computed $c_n(t)$ until a stationary state could be reached after multiple reflections of the wavepacket on the lattice boundaries. Therefore, for α and β larger than 2 [see Figs. 4(c) and 5(c)] we obtained a sharp curve collapse thus implying that the wavepacket spreads ballistically before reaching the boundaries of the chain. Notice, however, that the collapse of the participation number data is less striking because this quantity is more affected by statistical fluctuations. For α *or* β less than 2, on the other hand, panels (a) and (b) of Figs. 4 and 5 there is clearly no collapse, thus suggesting a much slower electronic dynamics along the chain [22].

In general lines, our results show that chains with correlated disorder in both diagonal and off-diagonal terms can only support the presence of extended states once both sources of disorder display strong enough correlations, that is $\alpha, \beta > 2$. Still, it is very impressive that two competing and independent sources of noise allow for coherent transmission of electronic excitations through the chain. That could, for instance, find many applications in quantum communication protocols using solid-state devices [61]. Now, we evaluate the robustness of a quantum-state transfer protocol [42] against such generalized disorder sources.

First, let us make further assumptions towards the configuration of the system. We now consider a chain made up by $N + 2$ sites [described by the very same Hamiltonian in Eq. (1) now with $N \to N + 2$], such that the first and last one will act as, respectively, sender and receiver parties. For those, particularly, we set $\epsilon_1 = \epsilon_{N+2} = 0$ and $J_1 = J_{N+1} = g$ that is, disorder is only present along the communication channel itself (sites 2 to $N + 1$). The transfer scheme we employ here is based on the weak-coupling model [44,45,62] – usually worked out in the context of spin chains – where g is set several orders of magnitude weaker than the energy scale of the channel. That forces both end sites to span their own subspace, with a couple of eigenstates taking the form $|\psi^{\pm}\rangle \approx (|1\rangle \pm |N+2\rangle)/\sqrt{2}$ so that state transmission takes place via coherent dynamics between them after time $\tau \sim \pi/\delta\lambda$, with $\delta\lambda$ being the (usually very small) energy gap between those states. Naturally, nearly-perfect transmission shall be expected in ordered chains. If that is not the case, the presence of generalized disorder breaks down the mirror and particle–hole symmetries of the system thus damaging the effective two-body coupling between the ends of the chain [45].

We are now about to show that a high-fidelity quantum-state transfer protocol can actually be realized in the presence of correlated fluctuations, involving the whole channel. Let us outline the transfer protocol following the original proposal from Ref. [42]. Suppose that Alice wishes to send an arbitrary qubit $|\varphi\rangle_1 = a|0\rangle_1 + b|1\rangle_1$ to Bob, where $|0\rangle_i$ ($|1\rangle_i$) denotes the absence (presence) of an electron at site i. Then, she arranges for an initial state of the form $|\Psi(0)\rangle = |\varphi\rangle_1|0\rangle_2 \ldots |0\rangle_{N+2}$. By letting the system evolve following its natural Hamiltonian dynamics, she expects, in the best-case scenario, to have $|\Psi(\tau)\rangle = |0\rangle_1|0\rangle_2 \ldots |0\rangle_{N+1}|\varphi\rangle_{N+2}$ so Bob can properly retrieve the qubit. A measure for the figure of merit of the protocol can obtained by averaging the input fidelity over the whole Bloch sphere (for details, see [42]):

$$F(t) = \frac{1}{2} + \frac{|c_{N+2}(t)|}{3} + \frac{|c_{N+2}(t)|^2}{6}, \tag{6}$$

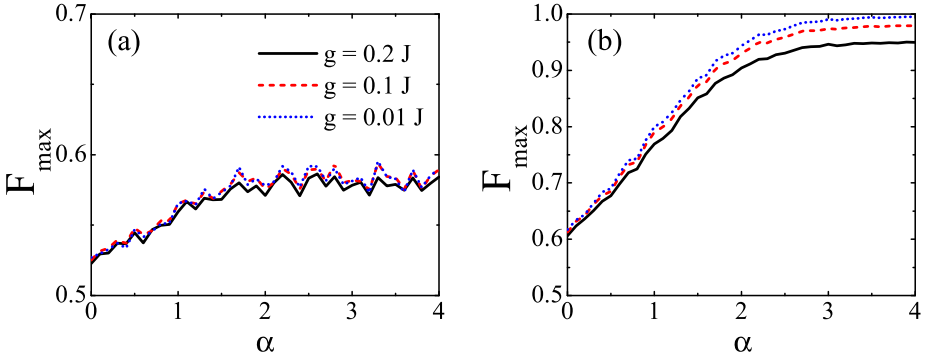

Fig. 6. Maximum fidelity versus α averaged over 500 independent realizations of disorder in a 50-site channel (52 sites total) for (a) $\beta = 0$ and (b) $\beta = 3$. Solid, dashed, dotted lines display results for $g/J = 0.2, 0.1, 0.01$, respectively. $F_{\max} \equiv \max\{F(t)\}$ was evaluated over the time window $tJ \in [0, 2 \times 10^5]$.

which is basically a monotonic function of the transition amplitude between sender and receiver sites, $c_{N+2}(t) \equiv \sum_j f_1^{j*} f_{N+2}^j e^{-iE_j t}$ [cf. Eq. (4)].

Here we are concerned with the maximum fidelity $F_{\max} = \max\{F(t)\}$ achieved during a given interval since the dynamics time scale of the system varies considerably from sample to sample. In particular, we evaluated $F_{\max}$ over $tJ \in [0, 2 \times 10^5]$ for about 500 independent realizations of disorder and averaged them out for every system configuration as shown in Fig. 6. There, it is clear that an efficient transfer protocol can be performed through such noisy channel once supported by prominent intrinsic correlations in both sources of disorder [see Fig. 6(b)]. We observe that $F_{\max}$ tends to saturate after $\alpha > 2$, thus pointing out the crucial role of extended states in the process. We also highlight in Fig. 6(b) that we are able to achieve nearly perfect fidelities provided g is weak enough, in order to avoid mixing between the channel and sender/receiver subspaces.

What is most impressive in the results shown above is that, even though the noisy channel must be augmented with strong long-range correlations in order to establish successful quantum-state transfer rounds, considerable amounts of global disorder are *still* present in the system due to the random nature of the phases used to generate the potential landscape. That ultimately destroys the mirror and particle–hole symmetries of the spectrum [54] and so, intuitively, it should not allow for an effective *resonant* interaction between the outer ends of the chain. Fortunately, it actually does. A very useful picture of this can be put forward by writing down the sender/receiver decoupled Hamiltonian with renormalized parameters obtained through second-order perturbation theory in g [(for details, see Ref. [45]), $H_{\text{eff}} = h_1|1\rangle\langle 1| + h_{N+2}|N+2\rangle\langle N+2| - J'(|1\rangle\langle N+2| + \text{h.c.})$, where

$$h_1 = -g^2 \sum_k |f_2^k|^2 / E_k, \tag{7}$$

$$h_{N+2} = -g^2 \sum_k |f_{N+1}^k|^2 / E_k, \tag{8}$$

$$J' = g^2 \sum_k f_2^k f_{N+1}^{k*} / E_k, \tag{9}$$

with the sum in k running over the normal modes of the channel only. Recalling that sites 1 (sender) and $N+2$ (receiver) are tuned to the middle of the band, $\epsilon_1 = \epsilon_{N+2} = 0$, the existence of delocalized states at this region of the spectrum provided the degree of correlations α and β are high enough (that is, greater than 2) is such that it *masks* the overall asymmetric nature of the chain yielding rather balanced distributions of amplitudes f_2^k and f_{N+1}^k. Hence, $h_1 \approx h_{N+2}$ what triggers an effective two-site dynamics with negligible local impurities. Moreover, since the renormalized parameters [Eqs. (7) through (9)] scales with E_k^{-1}, the outskirts of the band, filled by localized-like states (thus more spatially asymmetric), have a much weaker influence on them.

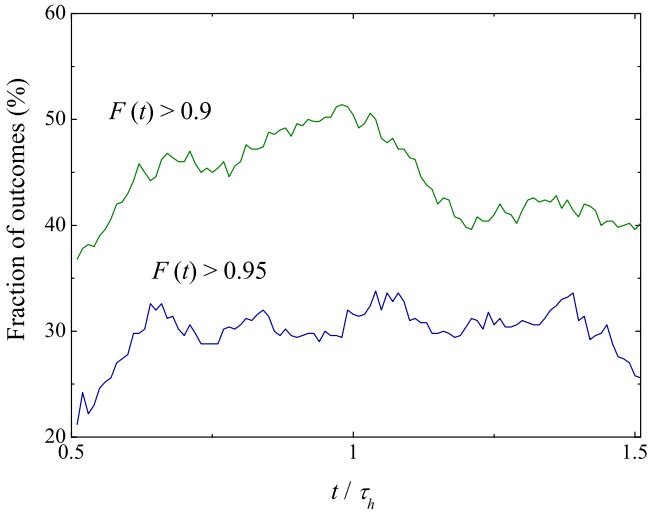

Fig. 7. Fraction of samples (%) satisfying $F(t) > 0.9$ and $F(t) > 0.95$ versus time in units of $\tau_h = \pi J/g^2$. We gathered 500 independent disorder realizations for $\alpha = 4$, $\beta = 3$, $N = 50$, and $g = 0.01J$.

3.3. Timing

Previously, we discussed the state-transfer figure of merit by focusing on the fidelity statistics over a fixed time interval. That allowed us to evaluate the prospect of generating an effective two-state (Rabi-like) dynamics between the first and last sites of the chain under the influence of long-range-correlated disorder. On the practical side, though, one should let Bob know in advance the time (at least approximately) the state is supposed to arrive at his location. Disorder, however, will unavoidably lead to timing errors unless precise knowledge over the configuration of the chain at every realization is available. Still, it is convenient to establish a proper measurement time window with higher chances of getting the state intended to, compatible to the type of disorder present in the system.

To see about that, let us first discuss how the transfer time responds to the hopping strengths of the chain. We recall that the transfer time for the effective two-site model is given by $\pi/\delta\lambda$, with the gap $\delta\lambda = 2|J'|$ [see Eq. (9)]. Given a uniform distribution of on-site potentials (that is, $\epsilon_n = \epsilon$) in a channel featuring an even number of sites N, it has been shown in Ref. [62] that the effective coupling J' between the outer ends of the chain can be expressed through a surprisingly simple formula (see [62] for details),

$$J' = g^2 \frac{J_3 J_5 \cdots J_{N-1}}{J_2 J_4 \cdots J_N} (-1)^{\frac{N}{2}} \tag{10}$$

Therefore, we readily see that for homogeneous couplings, say $J_i = 2J$ above, the transfer time is $\tau_h = \pi J/g^2$. Taking our disorder configuration into account, we expect that the transfer time τ associated with higher fidelities (close to unity) falls within the vicinity of τ_h.

Fig. 7 shows the fraction of samples displaying $F(t) > 0.9$ and $F(t) > 0.95$ at times ranging from $t = 0.5\tau_h$ to $t = 1.5\tau_h$. We readily note that about 50% of the disorder realizations had fidelities above 0.9 at specific times close to τ_h. Upon increasing this threshold to 0.95, the fraction reaches slightly over 30%. This is expected because the fidelity here is largely an oscillating function and so as we look towards the peak at some well defined time, the number of samples satisfying the threshold will decrease.

Last, we mention that, on the one hand, quantum communication protocols via weak-coupled ends [44,45,62] requires characteristically long times to perform the transfer when compared to

fully-engineered schemes [43]. On the other hand, it is shown to be very robust against static perturbations [55]. The transfer time can be substantially shortened by optimizing the outer couplings in order to achieve the so-called ballistic regime for quantum-state transfer [63]. The influence of correlated disorder on this regime is a subject worth to investigate in the future.

4. Conclusions

In this work we considered an electronic tight-binding chain with correlated disorder in both diagonal and off-diagonal terms of the Hamiltonian. The fractional Brownian motion was used to generate each corresponding disorder distributions. We analyzed the localization properties of the system, accounted by the participation ratio of its entire spectrum, and also evaluated the electronic dynamics profile along the chain. We showed that such model supports extended states only if both sources of disorder contain strong intrinsic long-range correlations with both $\alpha > 2$, and $\beta > 2$. We also investigated a possible application for this class of chains in the context of quantum-state transfer protocols. By perturbatively coupling both communicating parties to the noisy chain, it is possible to transmit an excitation from one end of the chain to another with very high fidelities as long as a proper set of delocalized states is available in the spectrum in order to overcome the spatial asymmetry induced by disorder.

By tackling the properties of a standard electronic hopping model augmented with twofold long-range-correlated disorder, we set the ground for further studies along that direction involving other classes of many-body interacting models. Moreover, we also highlight the importance of investigating special types of disorder that might occur in real solid-state devices for quantum information processing tasks [40].

Acknowledgments

This work was partially supported by CNPq (Grant No. 152722/2016-5), CAPES, and FINEP (Federal Brazilian Agencies), CNPq-Rede Nanobioestruturas, and FAPEAL (Alagoas State Agency).

References

[1] E. Abrahams, P.W. Anderson, D.C. Licciardello, T.V. Ramakrishnan, Phys. Rev. Lett. 42 (1979) 673.
[2] B. Kramer, A. MacKinnon, Rep. Progr. Phys. 56 (1993) 1469.
[3] A. Nandy, B. Pal, A. Chakrabarti, Europhys. Lett. 115 (2016) 37004.
[4] W.W. Cheng, L.J. Zhang, L.Y. Gong, S.M. Zhao, Ann. Phys. 370 (2016) 67.
[5] A.M. García-García, Phys. Rev. Lett. 100 (2008) 076404.
[6] A. Rodriguez, L.J. Vasquez, R.A. Römer, Phys. Rev. B 78 (2008) 195106.
[7] M. Modugno, New J. Phys. 11 (2009) 033023;
C. Tian, A. Altland, New J. Phys. 12 (2010) 043043;
F. Dukesz, M. Zilbergerts, L.F. Santos, New J. Phys. 11 (2009) 043026;
R. Steinigeweg, H. Niemeyer, J. Gemmer, New J. Phys. 12 (2010) 113001;
Y. Krivolapov, L. Levi, S. Fishman, M. Segev, M. Wilkinson, New J. Phys. 14 (2012) 043047.
[8] V. Gasparian, A. Suzuki, J. Phys.: Condens. Matter 21 (2009) 405302.
[9] A. Rodriguez, L.J. Vasquez, R.A. Römer, Phys. Rev. Lett. 102 (2009) 106406.
[10] A. Rodriguez, L.J. Vasquez, K. Slevin, R.A. Römer, Phys. Rev. Lett. 105 (2010) 046403.
[11] G. Lemarié, H. Lignier, D. Delande, P. Szriftgiser, J.C. Garreau, Phys. Rev. Lett. 105 (2010) 090601.
[12] A. Rodriguez, L.J. Vasquez, K. Slevin, R.A. Römer, Phys. Rev. B 84 (2011) 134209.
[13] J.J. Krich, A. Aspuru-Guzik, Phys. Rev. Lett. 106 (2011) 156405.
[14] V. Gasparian, M. Cahay, E. Jódar, J. Phys.: Condens. Matter 23 (2011) 045301.
[15] Y. Zhao, S. Duan, W. Zhang, Phys.: Condens. Matter 24 (2012) 245502.
[16] G.P. Zhang, M. Gao, Y.Y. Zhang, N. Liu, Z.J. Qin, M.H. Shangguan, J. Phys.: Condens. Matter 24 (2012) 235303.
[17] J.C. Flores, J. Phys. Condens. Matter 1 (1989) 8471.
[18] D.H. Dunlap, H.L. Wu, P.W. Phillips, Phys. Rev. Lett. 65 (1990) 88;
L., H. -Wu, P. Phillips, Phys. Rev. Lett. 66 (1991) 1366.
[19] F.A.B.F. de Moura, M.L. Lyra, Phys. Rev. Lett. 81 (1998) 3735.
[20] F.A.B.F. de Moura, M.L. Lyra, Physica A 266 (1999) 465.
[21] F.M. Izrailev, A.A. Krokhin, Phys. Rev. Lett. 82 (1999) 4062.
[22] F.A.B.F. de Moura, M.D. Coutinho-Filho, E.P. Raposo, M.L. Lyra, Europhys. Lett. 66 (2004) 585.
[23] M. Unge, S. Stafstrom, Phys. Rev. B 74 (2006) 235403.

[24] I.F. dos Santos, F.A.B.F. de Moura, M.L. Lyra, M.D. Coutinho-Filho, J. Phys.: Condens. Matter 19 (2007) 476213.
[25] F. Domínguez-Adame, V.A. Malyshev, F.A.B.F. de Moura, M.L. Lyra, Phys. Rev. Lett. 91 (2003) 197402.
[26] F.A.B.F. de Moura, Eur. Phys. J. B 78 (2010) 335.
[27] W.S. Liu, T. Chen, S.J. Xiong, J. Phys. Condens. Matter 11 (1999) 6883.
[28] G.P. Zhang, S.-J. Xiong, Eur. Phys. J. B 29 (2002) 491.
[29] V. Bellani, E. Diez, R. Hey, L. Toni, L. Tarricone, G.B. Parravicini, F. Domínguez-Adame, R. Gómez-Alcalá, Phys. Rev. Lett. 82 (1999) 2159.
[30] V. Bellani, E. Diez, A. Parisini, L. Tarricone, R. Hey, G.B. Parravicini, F. Domínguez-Adame, Physica E 7 (2000) 823.
[31] H. Shima, T. Nomura, T. Nakayama, Phys. Rev. B 70 (2004) 075116.
[32] T.F. Assunção, M.L. Lyra, F. Domínguez-Adame, F.A.B.F. de Moura, Phys. Lett. a 375 (2011) 1048.
[33] H. Cheraghchi, S.M. Fazeli, K. Esfarjani, Phys. Rev. B 72 (2005) 174207.
[34] G. Schubert, A. Weiße, H. Fehske, Physica B 801 (2005) 359.
[35] F.M. Izrailev, A.A. Krokhin, N.M. Makarov, Phys. Rep. 512 (2012) 125.
[36] A. Croy, M. Schreiber, Phys. Rev. B 85 (2012) 205147.
[37] C. Albrecht, S. Wimberger, Phys. Rev. B 85 (2012) 045107.
[38] G.M. Petersen, N. Sandler, Phys. Rev. B 87 (2013) 195443.
[39] P. Thiessen, E. Diaz, R.A. Romer, F. Domínguez-Adame, Phys. Rev. B 95 (2017) 195431.
[40] G.M.A. Almeida, F.A.B.F. de Moura, T.J.G. Apollaro, M.L. Lyra, Phys. Rev. A 96 (2017) 032315.
[41] U. Kuhl, F.M. Izrailev, A. Krokhin, H.J. Stöckmann, Appl. Phys. Lett. 77 (2000) 633.
[42] S. Bose, Phys. Rev. Lett. 91 (2003) 207901.
[43] M. Christandl, M. Datta, A. Ekert, A.J. Landahl, Phys. Rev. Lett. 92 (2004) 187902.
[44] A. Wójcik, T. Łuczak, P. Kurzyński, A. Grudka, T. Gdala, M. Bednarska, Phys. Rev. A 72 (2005) 034303.
[45] A. Wójcik, T. Łuczak, P. Kurzyński, A. Grudka, T. Gdala, M. Bednarska, Phys. Rev. A 75 (2007) 022330.
[46] B. Chen, Y. Li, Z. Song, C.-P. Sun, Ann. Phys. 348 (2014) 278.
[47] S. Longhi, Ann. Phys. 345 (2014) 63.
[48] G.M.A. Almeida, F. Ciccarello, T.J.G. Apollaro, A.M.C. Souza, Phys. Rev. A 93 (2016) 032310.
[49] X.-P. Zhang, B. Chao, S. Hu, J. Zou, L.-A. Wu, Ann. Phys. 375 (2016) 435.
[50] J.I. Cirac, P. Zoller, H.J. Kimble, H. Mabuchi, Phys. Rev. Lett. 78 (1997) 3221.
[51] G. De Chiara, D. Rossini, S. Montangero, R. Fazio, Phys. Rev. A 72 (2005) 012323.
[52] D. Burgarth, S. Bose, New J. Phys. 7 (2005) 135.
[53] D.I. Tsomokos, M.J. Hartmann, S.F. Huelga, M.B. Plenio, New J. Phys. 9 (2007) 79.
[54] N.Y. Yao, L. Jiang, A.V. Gorshkov, Z.-X. Gong, A. Zhai, L.-M. Duan, M.D. Lukin, Phys. Rev. Lett. 106 (2011) 040505.
[55] A. Zwick, G.A. Álvarez, J. Stolze, O. Osenda, Phys. Rev. A 84 (2011) 022311.
[56] S. Ashhab, Phys. Rev. A 92 (2015) 062305.
[57] M.P. Estarellas, I. D'Amico, T.P. Spiller, Phys. Rev. A 95 (2017) 042335.
[58] G.M.A. Almeida, F.A.B.F. de Moura, M.L. Lyra, arXiv:1711.08553 [quant-ph], 2017.
[59] M.O. Sales, F.A.B.F. de Moura, Physica E 45 (2012) 97.
[60] R.P.A. Lima, M.L. Lyra, E.M. Nascimento, A.D. de Jesus, Phys. Rev. B 65 (2002) 104416.
[61] T.J.G. Apollaro, S. Lorenzo, F. Plastina, Internat. J. Modern Phys. B 27 (2013) 1345035.
[62] G.M.A. Almeida, Phys. Rev. A 98 (2018) 012334.
[63] L. Banchi, T.J.G. Apollaro, A. Cuccoli, R. Vaia, P. Verrucchi, Phys. Rev. A 82 (2010) 052321; New J. Phys. 13 (2011) 123006; T.J.G. Apollaro, L. Banchi, A. Cuccoli, R. Vaia, P. Verrucchi, Phys. Rev. A 85 (2012) 052319.